


Lamb mode-coupling constant in quantum-dot semiconductor lasers

Laurent Chusseau* and Arthur Vallet

IES, Université de Montpellier, CNRS, Montpellier, France

Mathieu Perrin, Cyril Paranthoën, and Mehdi Alouini

FOTON, Université de Rennes, INSA, CNRS, Rennes, France (Received 27 March 2018; revised manuscript received 17 September 2018; published 10 October 2018)

In 1964, W. E. Lamb introduced a mode-coupling constant C to characterize the stability of a dual-mode laser. Considering quantum-dot semiconductor lasers, we calculate analytically C in the framework of a rate-equation model, which includes both the homogeneous broadening of the quantum-dot emission and the dot-to-dot carrier exchange due to wetting-layer-assisted lateral coupling. Although first established using fully symmetric laser parameters for both modes, this result is then extended numerically to nonsymmetric parameters and shows that C remains unchanged when the gain/losses are adjusted so that the two laser modes are brought to oscillate simultaneously. Finally, C is shown to depend on two parameters only encompassing the pumping, the gain material mainly through the homogeneous broadening and the dot-to-dot carrier exchange, and the cavity design. Above laser threshold, the analytic result predicts a stable dual-mode behavior whatever the conditions but with a margin that decreases drastically close to lasing threshold or at small beating frequencies.

DOI: [10.1103/PhysRevB.98.155306](https://doi.org/10.1103/PhysRevB.98.155306)**I. INTRODUCTION**

Already used today in commercial products working at gigahertz frequencies, photonics promises to become a major technology in the field of terahertz communications [1]. The growing interest in this field is fed by the existence of reliable components already developed for optical telecommunications, mainly at $1.55\ \mu\text{m}$. However, such large frequencies entail strong constraints on the components. In particular, THz generation can be accomplished by superimposing two laser fields on a photomixer [1], typically a low-temperature-grown InGaAs photoconductor or a unitravelling carrier photodiode. New photonic sources have to be developed that must be powerful enough to yield a detectable THz power after conversion and transmission and also have a very low phase noise in the beatnote. Several technologies are being developed. For instance, very efficient sources of millimeter-wave or THz sources have been demonstrated using the beating of two independent stabilized lasers [2].

To go further, compact or integrated sources operating at $1.55\ \mu\text{m}$ would be ideal, especially if they do not require active stabilization. Making the two laser fields oscillate within the same device enhances the spectral purity of the generated THz beatnote since the two fields will see the same sources of noise, be it thermal, mechanical, or electrical. The phase noises of the two modes will therefore be correlated and cancel out to a great extent in the beating [3]. The phase noise of the generated THz wave will then be reduced as compared to that obtained through the beating of two independent lasers of the same spectral width. It has already been demonstrated that such a dual-mode laser with solid state active medium

reduces the need of external feedback control of the beating frequency [4] and can even easily accommodate a simple feedback loop leading to a very high spectral purity [5].

Integrated dual-mode semiconductor lasers with quantum-well (QW) active layer were built to satisfy such a need of stable and compact sources [6,7]. Nevertheless, they have to cope with mode competition that may kill any stable dual-mode operation except if strategies like separate pumping of two distinct gain regions are implemented [8–10], which limit the efficiency of the noise reduction. In a previous paper [11], we addressed the question of the stability of the dual-mode regime in QW and quantum-dots (QD) semiconductor lasers using rate equations. Within this framework, it was proven that only QD lasers can operate simultaneously on two distinct modes but the simultaneous action of dot-to-dot carrier exchange and homogeneous broadening was ignored, although they have been considered separately.

On one hand, it is well known that a stable simultaneous emission from the excited and ground states of QDs is possible [12]. Rate-equations models have been proposed that describe quite accurately this regime [13,14], but the spectral splitting between the two modes is too high for mm-wave or THz emission. A simultaneous emission between closer modes interacting strongly within the homogeneous broadening is needed for practical applications. On the other hand, recent experimental studies [15,16] evidenced a stable dual-mode emission in QD lasers. Moreover, Ref. [16] demonstrates the possible tuning over the wide frequency range of 0.28–30 THz covering almost the whole inhomogeneous broadening. It is therefore useful to reconsider the QD-laser mode stability in the unified framework of dual-mode solid-state lasers, with aim to help for growth and laser design.

*laurent.chusseau@ies.univ-montp2.fr

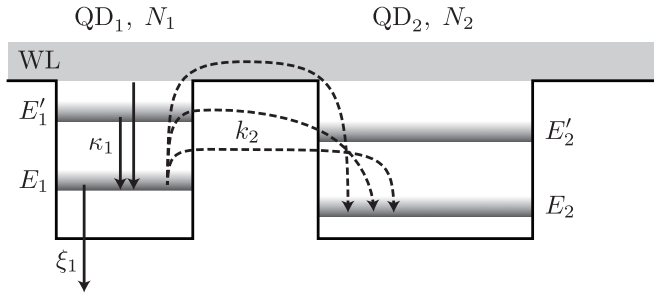


FIG. 1. Energy diagram representing some of the processes included in Eq. (4); the others are straightforwardly derived by symmetry. κ_i : nonresonant pumping; ξ_i : spontaneous recombination; k_i : exchange of carriers between dots. The distribution of QD is reduced to only two families, with resonance frequency separated by f , and interacting with two optical modes also separated by f . Each dot family interacts with its own resonant optical mode but also with the other detuned optical mode through the Lorentzian lineshape ϵ .

Since the earliest theory of gas lasers [17], the stability of the dual-mode regime is known to be governed by a simple constant. Mode intensities, I_1 and I_2 , follow the time evolution

$$\frac{dI_1}{dt} = (\alpha_1 - \beta_1 I_1 - \theta_{12} I_2) I_1, \quad (1a)$$

$$\frac{dI_2}{dt} = (\alpha_2 - \beta_2 I_2 - \theta_{21} I_1) I_2, \quad (1b)$$

where the α_i are unsaturated gains and β_i and θ_{ij} are self-saturation and cross-saturation coefficients. The stability analysis of this set of equations yields the expression of the Lamb coupling constant

$$C = \frac{\theta_{12} \theta_{21}}{\beta_1 \beta_2}. \quad (2)$$

The two modes oscillate simultaneously or not, depending on whether this constant is lower or higher than 1. Starting from the measurement technique of C proposed in Ref. [18], we derive in the following an analytical formulation of the coupling constant in the case of semiconductor QD lasers.

II. QD LASER MODEL

Unlike QW lasers where the optical gain of adjacent modes share exactly the same material gain, QDs have little interaction with each other once created. Moreover the total number of active QDs in resonance with a given optical mode is determined by the growth. To put them in an optically excited state, QDs have to capture free carriers from the barrier *via* the wetting layer (WL). Optical gain coupling between dots is thus not direct, which seems favorable for a stable dual-mode emission.

As a typical example of QD active layer, we will consider double cap InAs/InP QDs on InP(311)B for 1.55 μm optical emission [19]. QD dimensions are 30 nm in diameter and 3 nm in height above a one or two monolayers-thick InAs WL. Two adjacent QDs of different sizes are represented schematically in Fig. 1. In ascending energy order, above the QD fundamental transition, a doubly degenerated excited state has an energy about 50 meV higher, and another state may

be even less confined. At 100 meV above the fundamental transition starts a 2D continuum (miniband) for the WL, and roughly 100 meV above, states are delocalized in the InGaAsP barrier. These values are typical but may change with the exact growth conditions. In particular if QD density (QDD) increases, the excited states start to be coupled with those of neighboring QDs, leading to the delocalization of electronic states [20].

Due to the distribution of their sizes, QDs have a large inhomogeneous broadening of around 50 meV, i.e., 12 THz, that can be controlled to some extent [21]. We are considering the lasing of two optical modes, labeled 1 and 2, separated by a frequency difference f . They will interact with dots of different sizes. To keep our analysis simple, we consider only two QD families, also labeled 1 and 2 in Fig. 1, each one being resonant with its own optical mode. Therefore their center energies will be separated by hf . The homogeneous optical linewidth γ of a single QD is estimated between 12 meV and 20 meV FWHM at room temperature [22,23]. This provides a first coupling mechanism between both modes that can be accounted for using the parameter

$$\epsilon = \frac{1}{1 + (2hf/\gamma)^2} = \frac{1}{1 + 4\mathcal{F}^2}, \quad (3)$$

which is derived from the Lorentzian lineshape of the homogeneous gain of each QD family. If for instance family 1 provides a gain g for mode 1, it will also provide a gain ϵg for mode 2, where ϵ is comprised between 0 and 1. ϵ depends on the frequency splitting f of the two modes but also on QD growth conditions and confinement energy which influence the temperature and Auger broadening of the QD levels [23]. In our model, ϵ is the only parameter that accounts for the difference in frequency between modes. Although the beatnote frequency f is expressed in Hz, it will be useful and more practical to use the normalized frequency defined by $\mathcal{F} = hf/\gamma$, which scales according to the homogeneous broadening.

Another coupling mechanism has to be introduced that can operate in the absence of an optical cavity. Indeed, if carriers are injected in an excited state of a particular QD family, they will start to diffuse and thermalize with the other sublevels until recombinations occur. Several mechanisms can be considered, noted as dashed arrows in Fig. 1. The first one is a direct coupling between both ground states through the tunnel effect. For a typical in plane QD to QD separation of a few tens of nanometers—corresponding to QDD in the 10^{10} to 10^{11} cm^{-2} range—no ground state splitting due to lateral coupling of QDs has been predicted [20]. QD separation has to be in the range of few nanometers to create electronic coupling as evidenced in very close vertically coupled QD layers [24]. This effect on the ground state is thus expected to be weak and will not be considered in the following. The most probable path is, however, a thermionic excitation toward the first excited state followed by quantum tunneling to an adjacent QD. Under laser conditions, with high carrier density and ambient temperature, Auger scattering is well known to promote carrier redistribution and accelerate gain recovery in active QD devices [25]. Waiting times from and to the first excited state then fall in the ps range [26]. A tunneling redistribution via the WL assisted inter-QD coupling mechanism

was already evidenced in this system [20,27]. Its effectiveness obviously depends on the QDD that dictates the average distance between dots. The last mechanism corresponds to a complete thermionic emission to the wetting layer with a subsequent capture by the other QD family. This is not the dominant mechanism because of the energy difference between QD and WL levels, although the excited state may act as a relay.

Starting from multimode rate equations for semiconductor lasers [28] and QD lasers [13] we thus construct the following set of rate equations to encompass all these specific properties of a well above threshold QD dual-mode laser [11]

$$\frac{dN_1}{dt} = \kappa_1 + k_1 N_2 P_1 - k_2 N_1 P_2 - \xi_1 N_1 - A_1(N_1 - P_1)(S_1 + \epsilon S_2), \quad (4a)$$

$$\frac{dN_2}{dt} = \kappa_2 + k_2 N_1 P_2 - k_1 N_2 P_1 - \xi_2 N_2 - A_2(N_2 - P_2)(S_2 + \epsilon S_1), \quad (4b)$$

$$\frac{dS_1}{dt} = -\alpha_1 S_1 + (A_1(N_1 - P_1) + \epsilon A_2(N_2 - P_2))S_1, \quad (4c)$$

$$\frac{dS_2}{dt} = -\alpha_2 S_2 + (A_2(N_2 - P_2) + \epsilon A_1(N_1 - P_1))S_2, \quad (4d)$$

with $B_i = N_i + P_i$ the total number of QD addressing mode $i = 1, 2$, N_i the number of excited dots, P_i the number of unexcited dots, and κ_i the pumping per QD family. A_i , ξ_i , and α_i account for the modal gains, carrier leakage rates in the excited state, and linear optical losses per mode, including internal losses and external emission. The ϵ parameter already discussed takes into account the optical coupling between modes via Lorentzian gains. On the carrier side, coupling is obtained by the k_i 's that are constants accounting for the exchange rate of the excited states between the two QD families. Formally it is equivalent to adding another carrier equation for the wetting layer [13,29], but it is more convenient to manage and be consistent with the physical demonstration of direct coupling between QD families [20,27]. Practical numerical values for the k_i 's for a given fabrication process are still missing and surely depend on growth fabrication conditions like QDD. Nevertheless k_i values straightforwardly bind the two carrier population just like an action mass law. If moreover the optical gains differ significantly, the first population that reaches the laser threshold will progressively clamp all excited QD densities so that the other mode grows up with difficulty. This phenomenon causes the narrowing of the electroluminescence observed in Ref. [27] when QDD increases. As a result, the power balance between the two modes selected for beating may get lost. In the following we will assume close values for all laser parameters so as to preserve the dual-mode regime with nearly balance power between modes. It is worthwhile mentioning that this model assumes isotropic light-matter interaction. In the peculiar case where the two modes under consideration are orthogonally polarized, any gain anisotropy might lead to a polarization dependent coupling constant. This dependence was observed in a (100)-cut Nd:YAG laser where the active atoms cross sections are oriented according to the crystallographic axis [30]. This was also discussed in the VCSELs and modelled

with rate equations resembling Eq. (4) [31]. Here, irrespective of the polarization nature of the two modes, we shall consider that the light interaction with the QDs is quasi-isotropic in agreement with the fact that their random distribution yields a quasi-isotropic photoluminescence. Moreover, the short time scale of electronic spin coherence at room temperature is expected to randomize polarization dependent interactions [32,33].

The above model allows estimating straightforwardly the steady-state solutions for S_1^{ss} and S_2^{ss} using mathematical software [34]. Multiple solutions are obtained when solving for steady state [35]. The relative complexity of our rate-equation set (4) leads to seven roots [36]. Two of them are for the nonlasing regime ($S_1 = S_2 = 0$) within which only one is physically sound with positive quantum-dot numbers ($N_i > 0$). Besides, two solutions correspond to one lasing mode only, the valid root in each case corresponding to a positive number of photons. Finally only one solution yields simultaneously $S_1 > 0$ and $S_2 > 0$. This solution is selected for further analysis of the dual-mode regime. It must be noted that within this solution the simultaneous oscillation of the two modes has to be assessed by stability analysis [17,35].

III. LAMB CONSTANT

The experimental procedure used to extract the Lamb constant C involves a modulation of optical losses for each mode sequentially while recording the intensity evolution of the two modes [18]. Within the framework of our rate-equation model, optical intensities are proportional to S_i^{ss} and the losses are given by α_i . The intensity variation of mode 1 while modulating the losses of mode 2 is thus given by $dS_1^{\text{ss}}/d\alpha_2$ and should be divided by the modulated intensity of mode 2 in the same condition $dS_2^{\text{ss}}/d\alpha_2$. The converse applies when modulating the linear gain of mode 1. With the notations of Ref. [18], it yields

$$C \equiv K_{12}K_{21}, \quad (5)$$

with

$$K_{ij} \equiv -\frac{dS_i^{\text{ss}}}{d\alpha_j} \left(\frac{dS_j^{\text{ss}}}{d\alpha_j} \right)^{-1}. \quad (6)$$

A. Perfect symmetry between the two modes

We consider here closely separated modes of similar intensities. Moreover, we choose similar material and optical parameters for almost all variables except the losses α_i that must be kept different to evaluate C . This eventually arises when choosing two modes symmetrically located with respect to the inhomogeneous gain maximum. It yields $k_i = k$, $\kappa_i = \kappa/2$, $A_i = A$, $B_i = B$, and $\xi_i = \xi$. The steady-state number of excited quantum dots in each set i simply becomes

$$N_i^{\text{ss}} = \frac{B}{2} + \frac{\alpha_i - \alpha_j \epsilon}{2A(1 - \epsilon^2)}, \quad (7)$$

with $j \neq i$. In spite of the large number of simplifications brought by this complete symmetric case, the expressions for

the resulting S_i^{ss} remain quite complex [36]. For instance

$$S_1^{\text{ss}} = \frac{\kappa - B\xi}{2} f_- - \frac{kB(\alpha_1 - \alpha_2)}{2A(1 - \epsilon)} f_+ - \frac{\xi}{2A(1 + \epsilon)}, \quad (8)$$

where f_+ and f_- are functions of α_1 and α_2 :

$$f_{\pm}(\alpha_1, \alpha_2) = \frac{1}{\alpha_1 - \epsilon\alpha_2} \pm \frac{\epsilon}{\alpha_2 - \epsilon\alpha_1}. \quad (9)$$

The intensity of the second mode S_2^{ss} can be recovered by exchanging the indexes $1 \leftrightarrow 2$.

We then expand the derivatives in (6) using the previous expressions of S_i^{ss} . Once analytically evaluated, further simplifications can be obtained by assuming at that point identical losses, $\alpha_i = \alpha$. Equations are made completely symmetric and yield simpler expressions, for instance the common value for the mode intensities becomes

$$S_1^{\text{ss}} = S_2^{\text{ss}} = \frac{1}{2} \left[\frac{\kappa - B\xi}{\alpha} - \frac{\xi}{A(1 + \epsilon)} \right], \quad (10)$$

with the lasing threshold $\kappa_{\text{th}} = B\xi + \alpha\xi/A(1 + \epsilon)$, and both K constants become equals: $K_{12} = K_{21} = K$. Although violent in some sense, such an approximation is usually proposed and was proven to be compliant with experimental results. It was, for instance, shown experimentally in Er,Yb:glass as well as Nd:YAG lasers that the relevant parameter for dual-mode oscillation is C independently of K_{12} and K_{21} which can evolve with respect to wavelength but in opposite directions so that their product remains constant [37]. This approximation was also proposed in Ref. [38] to extract the value of the coupling constant C from spectral noise measurements in optically pumped Er:Yb:glass microchip lasers. It was also used in Ref. [30] to quantify polarization mode-coupling in Nd:YAG. After some manipulations [36] we end up with exactly the same equation as in Ref. [38]

$$C = \left[\frac{1 - (\Omega_L/\Omega_R)^2}{1 + (\Omega_L/\Omega_R)^2} \right]^2, \quad (11)$$

where

$$\frac{\Omega_L}{\Omega_R} = \frac{1 - \epsilon}{1 + \epsilon} \sqrt{\frac{a}{2 + a}},$$

and with the parameter $a = A(1 + \epsilon)(\kappa - B\xi)/(kB\alpha)$ that can be recast in the simpler form $a = \xi g_0/(kB\alpha)$, by introducing the unsaturated gain g_0 .

This result is surprisingly simple as compared to the lengthy steady-state forms (8), (9) extracted from rate equations. Furthermore, two key parameters only are needed to define the Lamb C constant; the first one is the homogeneous lineshape ϵ and the second is a . In the expression of a , ξ , and kB are rates related to the material, and g_0 and α are related to the laser design and operating point. For the material-related rates, $2kB$ is the rate at which the population difference $N_1 - N_2$ is null. Indeed, going back to Eqs. (4) and dropping the gain terms: $S_1 = S_2 = 0$; it can be shown that an initial difference $N_1 - N_2$ will evolve as $\exp(-2kbt)$, while $N_1 + N_2$ evolves as $\exp(-\xi t)$.

As $a > 0$ above threshold and $0 \leq \epsilon \leq 1$ the stability condition $C < 1$ is always fulfilled except when the two modes have exactly the same frequency ($f = 0$, or $\epsilon = 1$, will always give $C = 1$). This confirms our previous proof

of unconditional stability of QD dual-mode lasers that was however restricted to the nonsimultaneous consideration of homogeneous broadening and carrier exchange [11]. In more detail, as K_{12} and K_{21} are exactly the fraction within the brackets in (11), they are therefore always positive. It agrees with the out-of-phase evolution of the intensities experimentally observed when one modulates the losses of one mode [18]. In the framework of our model, the positive value of K_{ij} can be understood by the mode competition addressing the same QD population within the homogeneous broadening.

Although $C < 1$ theoretically leads to a possible dual-frequency operation, in practice a security margin must be applied to ensure its robust operation whatever the experimental variations that may arise because of thermal variations or mechanical instabilities. A more suitable maximum value for C is thus probably 0.95 for practical reasons since a stable dual-mode regime was already observed at this C level [18]. The value of C is always strictly decreasing with a , going from $C = 1$ for $a \rightarrow 0$ to $C = [2\epsilon/(1 + \epsilon^2)]^2$ for $a \rightarrow +\infty$. In order for the coupling constant to remain under a given value C , one should therefore take $a \rightarrow +\infty$ and $\epsilon < \epsilon_{\text{max}} = [1 - \sqrt{1 - C}]/\sqrt{C}$. Taking $C = 0.95$ as a limit yields $\epsilon_{\text{max}} = 0.80$ or $\mathcal{F} > 0.253$. Therefore, even if a dual-frequency operation is theoretically possible as soon as $\mathcal{F} \neq 0$, it should be quite difficult to achieve a beatnote at a frequency difference below one quarter of the homogeneous linewidth without artificially uncoupling the two modes.

Figure 2(a) shows the evolution of C as a function of \mathcal{F} , the beatnote frequency normalized to the homogeneous linewidth, and of the parameter a described above. The most favorable situation for robust dual-mode operation is when both a and \mathcal{F} are large. Looking at the contour curve corresponding to $C = 0.95$, it can be noticed that the minimum \mathcal{F} available barely increases when a is lowered from $+\infty$ down to $a = 0.5$. Below this value, only well separated modes are predicted to oscillate in a robust manner.

Figure 2(b) details the evolution of C with frequency over a wide range of normalized frequency corresponding to 6THz when the homogeneous broadening is 10 meV. Four values of a are considered and the evolution of C looks like a Lorentzian profile on top of a constant, which is easily estimated at $1/(1 + a)^2$. Increasing a is therefore of great importance. As the ratio g_0/α enters the definition of a , increasing the pumping power seems in principle an easy solution. However, care should be taken because the homogeneous linewidth is also expected to increase linearly with pumping power due to Auger broadening [23]. To contain this effect, the temperature should be lowered as it has an effect both on the phonon—predominant at low carrier densities—and on the Auger—predominant at large carrier densities—broadening of the levels [23].

Additionally, lowering the temperature will limit the exchange of carriers between dot families given by the rate kB . This parameter is the least well known in the expression of a . Although the interdot exchange of carriers was reported in some references dealing with QD laser equations [14], the value is often not given explicitly, or it is given in the framework of a continuous distribution of QD not amenable to analytic expressions. To give some hints, let's suppose that we want $a \geq 0.5$ at threshold ($g_0 = \alpha$). This will be possible even

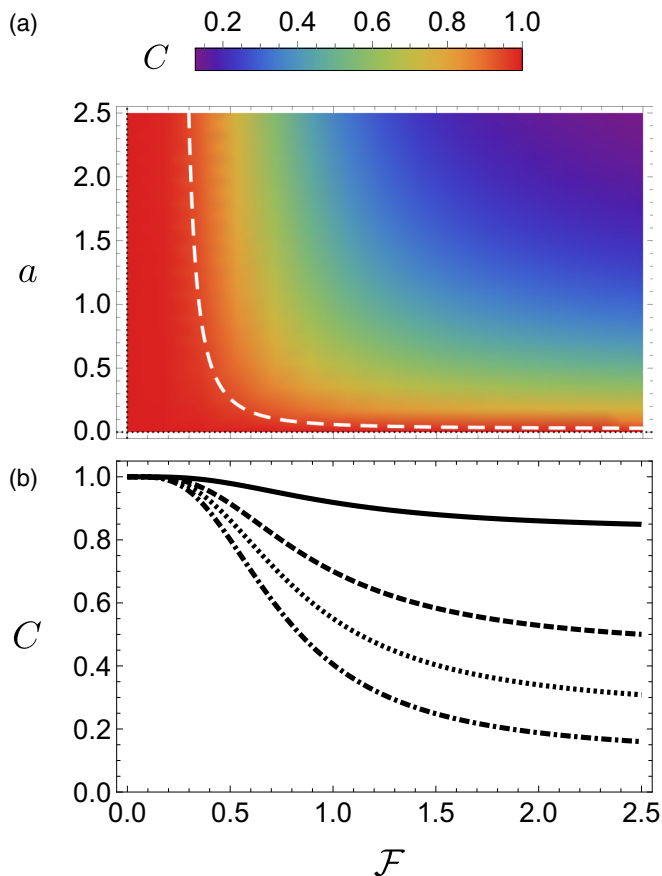


FIG. 2. (a) Values of the coupling constant C of a semiconductor QD laser in the (a, \mathcal{F}) plane as well as the particular contour line corresponding to $C = 0.95$ (white dashed curve). (b) Calculated Lamb constant C as a function of \mathcal{F} . Four a values are considered: $a = 0.1$, solid line; $a = 0.5$, dashed line; $a = 1$, dotted line; $a = 2$, dash-dotted line.

if the transfer rate kB is as large as 2ξ , or if a carrier present in a particular QD has twice more chances to be transferred to an empty QD from the other family than to recombine within the QD. To reduce the impact of carrier exchange, the barrier height should be made as large as possible and the QDD lowered. Alternatively, it may be possible to separate the layers, introducing a barrier between the layer of the larger dots and that of the smaller dots.

B. No symmetry between the two modes

Previous considerations have focused on the very singular case of perfect symmetry between modes for both gains and losses. This leads to simplifications for steady-state values, which enable analytical calculus and thus to draw some trends for the coupling constant value. It is important to show here, by numerical calculations, that the C consistency shown for Er,Yb:glass as well as Nd:YAG lasers is still valid for QD lasers. This will thus reinforce the generality of Eq. (11).

By returning to the general solutions calculated in §II and considering more specifically the steady-state dual-mode solution, we estimated the limits where either of the S_i^{SS} vanishes with the only assumption that the two modes are

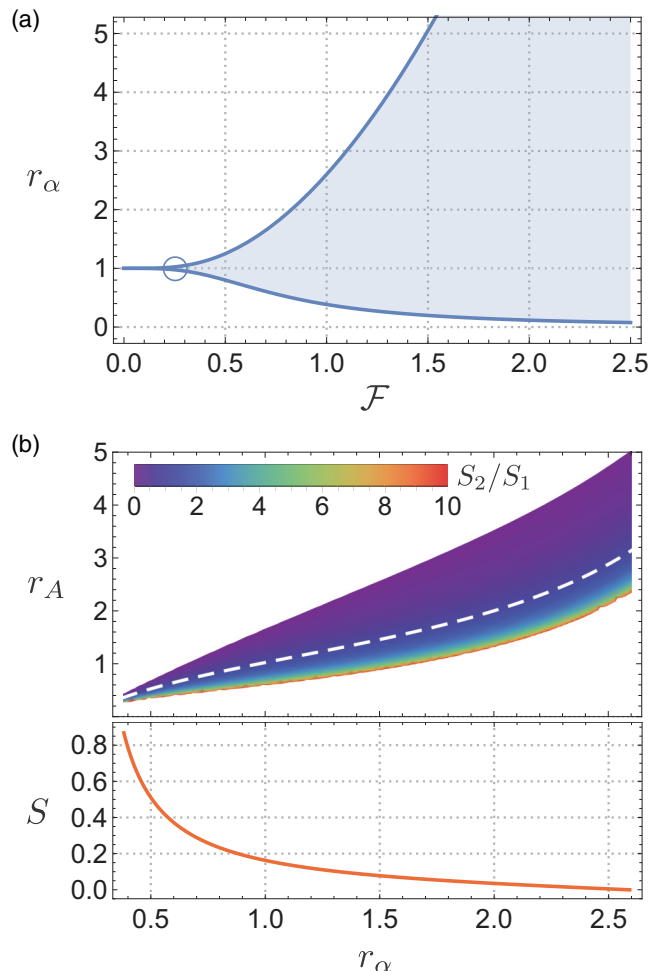


FIG. 3. Common parameters are $\mathcal{F} = 1$, $a = 2$, and $kB/\xi = 0.2$. (a) Limiting curves of steady-state dual mode as a function of the normalized frequency and $r_\alpha = \alpha_1/\alpha_2$, the ratio of optical mode losses. The area between the curves is the allowed region, here obtained at high pumping level, and the circle figures the $\mathcal{F} > 0.253$ introduced for $C \geq 0.95$. (b) Up: Power intensity ratio between modes, S_2/S_1 , as a function of r_α and $r_A = A_2/A_1$, the gain ratio of the two modes. The r_α span extends over the allowed area defined in (a) for $\mathcal{F} = 1$. The dashed white line figures the solution $S = S_1 = S_2$ of perfect balance between mode intensities while white areas correspond to (r_α, r_A) pairs where the dual-mode regime vanishes. Down: Example of the common normalized intensity of the two modes S calculated along the white dashed curve; other parameters are here $A = 10 \text{ ns}^{-1}$, $B = 10^4$, $\xi = 0.1 \text{ ns}^{-1}$, and $\alpha = 0.01 \text{ ns}^{-1}$.

pumped identically ($\kappa_1 = \kappa_2 = \kappa/2$). For convenience, the parameter $r_\alpha = \alpha_1/\alpha_2$ is introduced. If we assume a large pumping level, mathematically if it tends towards infinity, the range allowed for r_α is radically simplified [36]

$$\frac{2\epsilon}{1 + \epsilon^2} < r_\alpha < \frac{1 + \epsilon^2}{2\epsilon}. \quad (12)$$

Outside this domain, at least one of the S_i^{SS} is negative so the first required condition for dual-mode operation is excluded. Figure 3(a) gives a representation of that domain in the (\mathcal{F}, r_α) plane together with the position of the previously discussed limit $C = 0.95$ in the fully symmetric case. Although the

possible asymmetry between the losses of the two modes is negligible at low frequency, the range of r_α values opens quickly at high frequency, which facilitates dual-mode operation. The $C \leq 0.95$ limit given above appears as the reference value at which the very restrictive condition of very close losses in both modes is relaxed.

In practice, proper dual-mode operation is obtained by counterbalancing possible gain anisotropy with loss anisotropy so that the two mode intensities are equal. The operator tries to equalize S_1^{SS} and S_2^{SS} either by pumping the two modes differently or by adjusting the losses. In QD lasers shifting the two modes in frequency beyond the homogeneous broadening width might be an attractive alternative.

By introducing the ratio between the differential gains $r_A = A_2/A_1$, it is then possible to solve for $S_1^{SS} = S_2^{SS} = S$ in the steady state and to preserve the equality between mode intensities. We do so assuming that $k_i = k$, $\kappa_i = \kappa/2$, $\xi_i = \xi$, $B_i = B$ but $\alpha = \alpha_1 = r_\alpha \alpha_2$ and $A = A_1 = A_2/r_A$. Because of these definitions, r_α decreases if the operator adds losses on mode 2 with respect to mode 1 and obviously r_A must also decrease in order to balance the emission between the two modes. The upper part of Fig. 3(b) plots the power intensity ratio $r_S = S_2^{SS}/S_1^{SS}$ in the (r_α, r_A) plane for the allowed r_α values defined by (12). The area allowed for an actual positive ratio is limited in space and includes the condition $r_S = 1$ as a white dotted line. This illustration uses numerical solutions that also require a known value of the ratio between the carrier's exchange rate, kB , and the nonradiative spontaneous recombination rate ξ . Here we chose $kB/\xi = 0.2$. Numerical solutions predict r_S ratios that increase dramatically as we approach the lower edge of the allowed area; we have limited its value to $r_S \leq 10$ in the graph. Obviously, the perfect symmetry $r_\alpha = r_A = 1$ belongs to the $r_S = 1$ curve.

The laser pumping being constant, when the gain and losses are adjusted the intensities on both modes are subject to change. The lower part of Fig. 3(b) illustrates this change when located on the white dotted line $r_S = 1$. Although the vertical scale is subject to change depending on the actual laser parameters, the steady decrease of S from high values at low r_α to zero at its upper limit is a reproducible behavior. Therefore, even if each pair (r_α, r_A) on the white dotted line balances the intensities, the total power emitted by the laser is likely to change.

Using the full steady-state expressions of S_i^{SS} discussed in §II and the definitions of (5) and (6), we are now able to numerically calculate C , K_{12} , and K_{21} assuming the balanced condition is met, i.e., assuming for each set of parameters a pair (r_α, r_A) located on the white dashed line of Fig. 3(b), knowing that the latter must be recalculated each time the laser parameters are modified. Such a procedure is intended to reproduce what an experimenter does when trying to adjust the losses and gains of his laser as in Ref. [18] to preserve the dual-mode regime. The results are given in Fig. 4 with four examples corresponding to various parameters \mathcal{F} , a , kB/ξ . They are all plotted over a range of r_α which corresponds exactly to the allowed area previously defined in Fig. 3(a).

For all laser conditions, C remains below the stability limit of unity while the K_{ij} have opposite evolutions and cross at the symmetric conditions $r_\alpha = 1$. It is worth noting that C has negligible amplitude variations as compared to those of

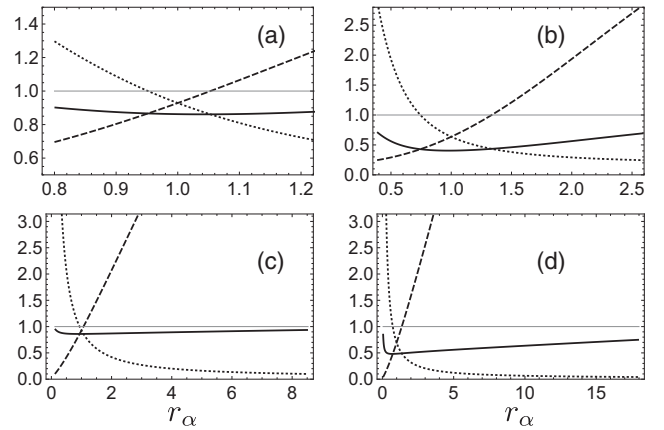


FIG. 4. Lamb constant C (solid line), K_{12} (dashed line), and K_{21} (dotted line) as a function of r_α while ensuring at each point that mode intensities remains balanced by a proper adjustment of $r_A = A_2/A_1$. Parameters are (a) $\mathcal{F} = 0.5$, $a = 1$, $kB/\xi = 0.5$, (b) $\mathcal{F} = 1$, $a = 2$, $kB/\xi = 0.2$, (c) $\mathcal{F} = 2$, $a = 0.1$, $kB/\xi = 2$, (d) $\mathcal{F} = 3$, $a = 0.5$, $kB/\xi = 1$. The thin continuous line is an eye guide @ $C = 1$.

K_{12} and K_{21} . This is especially true at higher frequencies where the range of r_α is large [Figs. 4(c) and 4(d)], which gives a difference between K_{ij} that can become important while C remains fairly constant. As discussed in Fig. 3(b), the intensities of the two modes are analytically related and depend on both r_α and r_A , with the consequence that the total laser power at both ends of the r_α range is not identical to that obtained for example for fully symmetrical conditions, and even ends up going to zero at one of the extremes of this variation. The consequence appears with changes on C appearing mainly at these extremes, which we do not consider significant since the initial dual-mode laser has been modified too much. Therefore, Fig. 4 compares the values of C for lasers with two similar modes but with different total emitted power, especially in the (c) and (d) cases. Note that case (b) corresponds to that of Fig. 3(b), which gives an idea of the amplitude of variation of the total intensity in relation to r_α . Trying to solve the system simultaneously for balanced intensities and constant laser power would also have required a change in the pump intensity κ and the introduction of many more parameters, making any parametric analysis tremendously complicated.

Based on the results of Fig. 4 and on the experimental knowledge acquired on microchip lasers and VECSEL [18,39], we postulate that C is almost a constant for a given dual-mode configuration and comparable intensities, regardless of a slight change in losses on either mode. On the contrary, the K_{ij} , which are the ratio between cross- and self-saturation of the two modes, are highly dependent on this change. Under such conditions, the relation (11) for C seems to be much more general than the very specific conditions used for its demonstration. In its microchip laser version, the same equation was successfully applied “as is” to extract the C Lamb constant of dual-mode lasers in two experiments [30,38]. As soon as QD semiconductor VECSELS are built, the same characterization will be possible and its validation, for example, thanks to the measurement of Ω_L and Ω_R , is expected.

IV. CONCLUSION

We have analytically calculated the Lamb constant C of dual-mode semiconductor QD lasers. It is found to depend only on two parameters and is always less than one, the theoretical limit for unconditional dual-mode stability. Nevertheless, in practice the operation of such a laser may not be envisioned if C becomes too close of unity. The robustness of the dual-mode operation can be evaluated through the parameters governing the analytical form of C .

The first parameter a is a combination of material and of laser design parameters reflecting the fact that QD families are coupled both directly and through the cavity. It should be made as large as possible, typically larger than 0.5, to limit the coupling between the modes. The second parameter is quite directly the homogeneous broadening of QD emission, leading to gain overlap between adjacent modes.

The homogeneous broadening has the strongest influence when modes are very close in frequency and it is a true

limitation for microwave sources. Sources working at a beat-note frequency below 1THz will need a careful design of the homogeneous linewidth, which is in favor of using QD active media. Its influence can be mitigated by maximizing the a parameter.

At THz frequencies, less difficulties are expected because the optical gains of the two modes are sufficiently separated to effectively decouple the modes. Therefore, more integrated structures can be envisaged without the need of applying a spatial separation between the two modes and could even be hybridized with the photoconductive THz antenna in a very compact way.

ACKNOWLEDGMENTS

This work is supported by the French Agence Nationale de la Recherche under the Swiss-French IDYLIC contract ANR-15-CE24-0034.

-
- [1] T. Nagatsuma, G. Ducournau, and C. C. Renaud, *Nat. Photonics* **10**, 371 (2016).
 - [2] G. Ducournau, P. Szriftgiser, T. Akalin, A. Beck, D. Bacquet, E. Peytavit, and J. Lampin, *Opt. Lett.* **36**, 2044 (2011).
 - [3] S. De, G. Baili, S. Bouchoule, M. Alouini, and F. Bretenaker, *Phys. Rev. A* **91**, 053828 (2015).
 - [4] A. Rolland, G. Ducournau, G. Danion, M. Brunel, A. Beck, F. Pavanello, E. Peytavit, T. Akalin, M. Zakoune, J.-F. Lampin *et al.*, *IEEE Trans. Terahertz Sci. Technol.* **4**, 260 (2014).
 - [5] G. Pillet, L. Morvan, M. Brunel, F. Bretenaker, D. Dolfi, M. Vallet, J.-P. Huignard, and A. Le Floch, *J. Lightwave Technol.* **26**, 2764 (2008).
 - [6] M. Brunner, K. Gulden, R. Hovel, M. Moser, J. F. Carlin, R. P. Stanley, and M. Ilegems, *IEEE Photonics Technol. Lett.* **12**, 1316 (2000).
 - [7] L. Chusseau, G. Almuneau, L. A. Coldren, A. Huntington, and D. Gasquet, *IEE Proc. J* **149**, 88 (2002).
 - [8] N. Kim, J. Shin, E. Sim, C. W. Lee, D.-S. Yee, M. Y. Jeon, Y. Jang, and K. H. Park, *Opt. Express* **17**, 13851 (2009).
 - [9] C. Zhong, X. Zhang, L. Yu, J. Liu, W. Hofmann, Y. Ning, and L. Wang, *IEEE Photonics Technol. Lett.* **29**, 1840 (2017).
 - [10] H.-Z. Weng, Y.-Z. Huang, Y.-D. Yang, X.-W. Ma, J.-L. Xiao, and Y. Du, *Phys. Rev. A* **95**, 013833 (2017).
 - [11] L. Chusseau, F. Philippe, P. Viktorovitch, and X. Letartre, *Phys. Rev. A* **88**, 015803 (2013).
 - [12] A. Markus, J. X. Chen, C. Paranthoën, A. Fiore, C. Platz, and O. Gauthier-Lafaye, *Appl. Phys. Lett.* **82**, 1818 (2003).
 - [13] M. Sugawara, K. Mukai, Y. Nakata, H. Ishikawa, and A. Sakamoto, *Phys. Rev. B* **61**, 7595 (2000).
 - [14] Z. Lin, Z. Wang, and G. Yuan, *Phys. Rev. A* **92**, 013808 (2015).
 - [15] K. Akahane, N. Yamamoto, A. Kanno, K. Inagaki, T. Umezawa, T. Kawanishi, T. Endo, Y. Tomomatsu, and T. Yamanoi, *Appl. Phys. Express* **6**, 104001 (2013).
 - [16] K. A. Fedorova, A. Gorodetsky, and E. U. Rafailov, *IEEE J. Sel. Top. Quantum Electron.* **23**, 1 (2017).
 - [17] W. E. Lamb, *Phys. Rev.* **134**, A1429 (1964).
 - [18] M. Alouini, F. Bretenaker, M. Brunel, A. Le Floch, M. Vallet, and P. Thony, *Opt. Lett.* **25**, 896 (2000).
 - [19] P. Caroff, C. Paranthoen, C. Platz, O. Dehaese, H. Folliot, N. Bertru, C. Labbé, R. Piron, E. Homeyer, A. L. Corre, and S. Loualiche, *Appl. Phys. Lett.* **87**, 243107 (2005).
 - [20] C. Cornet, C. Platz, P. Caroff, J. Even, C. Labbé, H. Folliot, A. Le Corre, and S. Loualiche, *Phys. Rev. B* **72**, 035342 (2005).
 - [21] C. Paranthoen, N. Bertru, O. Dehaese, A. Le Corre, S. Loualiche, B. Lambert, and G. Patriarche, *Appl. Phys. Lett.* **78**, 1751 (2001).
 - [22] K. Matsuda, K. Ikeda, T. Saiki, H. Tsuchiya, H. Saito, and K. Nishi, *Phys. Rev. B* **63**, 121304(R) (2001).
 - [23] H. H. Nilsson, J.-Z. Zhang, and I. Galbraith, *Phys. Rev. B* **72**, 205331 (2005).
 - [24] M. Bayer, P. Hawrylak, K. Hinzer, S. Fafard, M. Korkusinski, Z. R. Wasilewski, O. Stern, and A. Forchel, *Science* **291**, 451 (2001).
 - [25] N. Majer, K. Lüdge, and E. Schöll, *Phys. Rev. B* **82**, 235301 (2010).
 - [26] P. Miska, J. Even, X. Marie, and O. Dehaese, *Appl. Phys. Lett.* **94**, 061916 (2009).
 - [27] C. Cornet, M. Hayne, P. Caroff, C. Levallois, L. Joulaud, E. Homeyer, C. Paranthoen, J. Even, C. Labbé, H. Folliot, V. V. Moshchalkov, and S. Loualiche, *Phys. Rev. B* **74**, 245315 (2006).
 - [28] M. Ahmed, *Physica D* **176**, 212 (2003).
 - [29] K. Veselinov, F. Grillot, C. Cornet, J. Even, A. Bekiarski, M. Gioannini, and S. Loualiche, *IEEE J. Quantum Electron.* **43**, 810 (2007).
 - [30] A. McKay, J. M. Dawes, and J.-D. Park, *Opt. Express* **15**, 16342 (2007).
 - [31] J. Albert, G. Van der Sande, B. Nagler, K. Panajotov, I. Veretennicoff, J. Danckaert, and T. Erneux, *Opt. Commun.* **248**, 527 (2005).
 - [32] M. San Miguel, Q. Feng, and J. V. Moloney, *Phys. Rev. A* **52**, 1728 (1995).
 - [33] S. De, V. Potapchuk, and F. Bretenaker, *Phys. Rev. A* **90**, 013841 (2014).
 - [34] *Wolfram Mathematica*, Wolfram Research Inc. (2017), version 11.2 <http://www.wolfram.com/mathematica/>.

- [35] K. Otsuka, P. Mandel, S. Bielawski, D. Derozier, and P. Glorieux, *Phys. Rev. A* **46**, 1692 (1992).
- [36] See Supplemental Material at <http://link.aps.org/supplemental/10.1103/PhysRevB.98.155306> for calculation details.
- [37] M. Alouini, Theoretical and experimental study of Er^{3+} and Nd^{3+} solid-state lasers: Application of dual-frequency lasers to optical and microwave telecommunications, Ph.D. thesis, University of Rennes 1, Rennes, 2001.
- [38] M. Brunel, A. Amon, and M. Vallet, *Opt. Lett.* **30**, 2418 (2005).
- [39] V. Pal, P. Trofimoff, B.-X. Miranda, G. Baili, M. Alouini, L. Morvan, D. Dolfi, F. Goldfarb, I. Sagnes, R. Ghosh *et al.*, *Opt. Express* **18**, 5008 (2010).